

ARTICLES

Pulsed Field Gradient NMR Study of the Diffusion of H₂O and Polyethylene Glycol Polymers in the Supramolecular Structure of Wet Cotton

B. Newling*

Department of Physics, University of New Brunswick, PO Box 4400, Fredericton, NB, E3B 5A3, Canada

S. N. Batchelor*

Unilever Research Port Sunlight, Quarry Road East, Bebington, Wirral CH63 3JW, Great Britain

Received: December 12, 2002; In Final Form: September 4, 2003

PFG NMR results are reported on H₂O, PEG200, PEG1500, PEG8000, and PEG20000 in wet cotton fibers and H₂O in wet cotton linters. The data are analyzed in terms of a two-site exchange model (water/cotton) and show that the probe molecules in fibers are trapped in cages. The cage size decreases from 10 to 2 μm as the probes' size increases from 0.23 to 9.2 nm, although the overall accessible volume only decreases from 50 to 20–30%. This behavior may be explained by size-exclusion effects on the connectivity and accessibility. Analysis of the diffusion coefficients at short diffusion times indicates that fiber cages are water pools held between the growth rings of the fiber. In linters these cages do not occur, and a freely diffusing signal from H₂O in the amorphous region is observed with $D = (4.5\text{--}8.9) \times 10^{-11} \text{ m}^2 \text{ s}^{-1}$, which when compared to the predicted value from the microviscosity of the amorphous regions gives a tortuosity of 2–4. Exit of all probes from linters and fibers takes 0.2 s and requires hydrogen bonds to be broken with an activation energy of 50 kJ mol⁻¹.

Introduction

Porous materials are crystalline or amorphous solids that allow the reversible passage of molecules through their structure.¹ Typical examples are zeolites with their regular network of nanopores and cages and fibers where the porosity arises from the amorphous regions in the structure. A particularly important fiber in this respect is cotton,^{2,3} which is man's most important clothing material and widely used in many medical applications. For the optimum use of all porous materials it is important to understand how/where molecules move in and out of the nanostructures so that their chemistry and physics may be predicted.

Cotton is a remarkably pure and well-defined material constructed of polysaccharide chains, which are packed into regularly arranged crystalline and irregular amorphous regions.^{2,3} The crystallites are approximately 5–7 nm wide and 9–12 nm long with amorphous pores of 1–5 nm width between them. These pores are filled with irregularly arranged sections of polysaccharide chains and water; they are readily accessible to external agents and occupy 42% of the volume. The crystalline/amorphous nanostructure is built up into microfibrils that are 10–100 nm in width and up to 10 μm in length. These microfibrils are parallel packed to construct the growth rings, which then form fibers of several cm in length and 20 μm in width. The basic structural units are illustrated in Figure 1. Much shorter cotton linters are constructed in a similar manner and

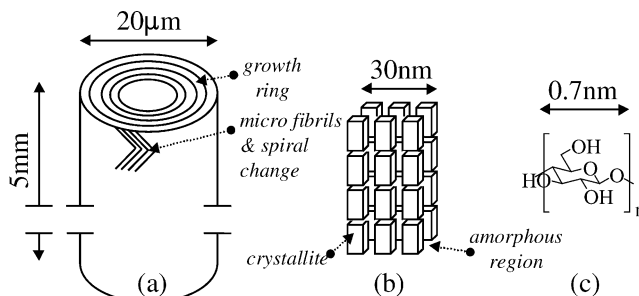


Figure 1. Schematic pictures of the cotton fiber and its components. (a) Cotton fiber constructed from growth rings, which are themselves constructed from microfibrils. Only a few of the growth rings and microfibrils are shown. (b) Microfibril, divided into amorphous and crystalline regions. Note that the amorphous region is not empty space but filled with disorganized polysaccharide chains and water. Its length (on the order of micrometers) is much larger than shown. (c) Basic unit of the polysaccharide chain.

form the so-called fuzz fibers of the plant. When saturated with water, the fiber shows great anisotropy in its swelling, increasing by 50% in its cross-section area but only 0.1% in its length. Linters show a similar anisotropy but increase only the cross-section area by 21%. In both cases the swelling is mainly due to water filling the space between the growth rings.

Recent electron paramagnetic resonance and flash photolysis work has probed the nature of the amorphous regions of cotton.^{4–8} A wide range of contemporary NMR techniques have also been applied to cellulose in general.^{9–13} Exact details of how/where molecules move in and out of cotton are not yet

* Corresponding authors. E-mail: bnewling@unb.ca; Stephen.Batchelor@unilever.com.

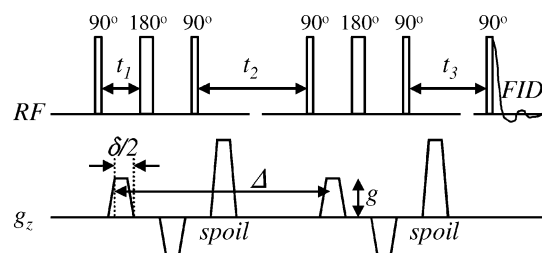


Figure 2. Pulse sequence timing for bipolar PFG measurements. The upper line shows the history of radio frequency (RF) pulse application and signal detection (the final free-induction decay). The lower line (g_z) shows the history of gradient application. The gradients labeled "spoil" are intended to destroy residual transverse magnetization in periods of magnetization storage (t_2 and t_3). The remaining bipolar gradient pairs provide motion sensitization (diffusion sensitization) to the sequence. The amplitude, g , of these pairs is stepped through 32 values to generate each of the curves shown in Figure 3. The gradient rise/fall times were 200 μ s, and the gradients were assumed to be trapezoidal for the calculation of $\delta = 2(\delta/2)$. Other timing parameters were typically $t_1 = 1.7$ ms (with the gradient pulse central to that interval), $t_3 = 5.3$ ms. t_2 varied with Δ .

known, despite this being an essential part of the drying, dyeing, and dirtying of cotton. To gain a better understanding, pulsed field gradient (PFG) NMR¹⁴ is an appealing technique, as it monitors the motion of probe molecules over the micrometer length scale, applicable to cotton suprastructure.¹⁵ Deviations from free liquid diffusion due to restricting geometry and exchange between compartments may be obtained by fitting the data to a model correlated to the known micro- and nanostructure. Here wet cotton fibers are investigated by this technique using H₂O and a series of poly(ethylene glycol) (PEG) polymers varying from 200 to 20 000 in molecular weight. Application of PEGs is new in this field and allows the effect of probe size on diffusion to be investigated. The probes chosen range from 0.23 to 9.2 nm in diameter, covering the sizes of the amorphous pores in cotton.¹⁶ PEGs also have the advantage of not undergoing proton exchange, removing possible exchange effects with the cellulose. Cotton linters are probed with H₂O to see if the much shorter fiber length affects the motion.

Experimental Section

Pulsed field gradient (PFG) NMR measurements were carried out at 7.2 T (300 MHz, ¹H) in an Oxford Magnet Technologies vertical, wide-bore superconducting magnet under the control of a Bruker DSX 300 solid-state console. The radio frequency probe and water-cooled gradient windings are a single unit (Bruker), with 5 mm internal diameter. Cotton samples were prepared in 5 mm NMR tubes. The maximum gradient that the unit can nominally apply is 10 T m⁻¹ (1 kG cm⁻¹). The measurements were made using a variant of the Cotts 13-interval bipolar PFG diffusion pulse sequence, which is illustrated schematically in Figure 2.^{17,18} The sequence is intended to minimize the errors due to sample-induced magnetic field inhomogeneities and eddy current in the gradient coil windings.^{19,20} The 90° and 180° pulse durations were optimized for each measurement, with typical values of 15 and 30 μ s, respectively. For all measurements, the elements of the bipolar gradient pair were identical in amplitude. The duration of gradient application, δ , was constant at 2.5 ms (taking the gradient pulses to be trapezoidal). The amplitude of the bipolar gradient pair, g , was stepped through 32 different values to generate each of the curves shown in Figure 3, and the diffusion time, Δ , varied to give a family of such curves (Figure 3). Data acquisition times were typically 1–8 h (involving 32–288

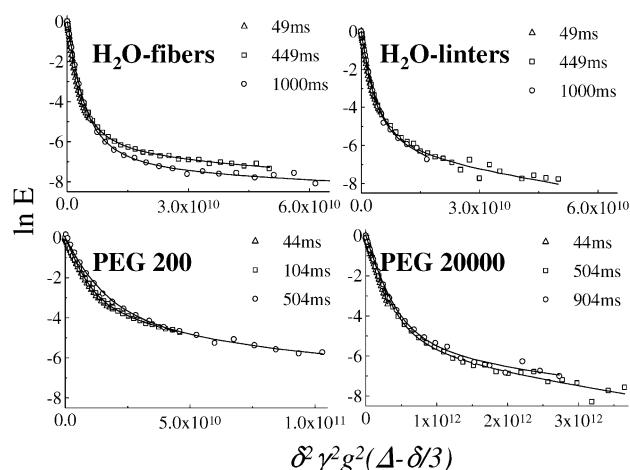


Figure 3. Experimental signal attenuation curves and their fits to Kärger model, eqs 2–5.

accumulations), for the shortest Δ and up to 35 h for the longest (up to 1248 accumulations). Similar data acquisition times were required for PEGs and water. All experiments were conducted at the bore temperature of 291 K.

In the water experiments cotton was placed in the NMR tube and soaked with excess water (demineralized H₂O), and the excess was then removed by syringe. This method meant that 1 g of cotton fibers was associated with 1.1 g of water and 1 g of linters with 1.3 g of water, taking into account the adsorbed water already in the air-dried fibers at lab humidities.² Figures are accurate to $\pm 20\%$. Thus all experiments were carried out with samples oversaturated with water. Cotton fibers were obtained by deconstructing pure unmercerized cotton sheeting from a commercial supplier (Phoenix Calico). Cotton linters were obtained from Aldrich and used as supplied. For the PEG experiments, 5% PEG solution in D₂O was used to wet the cotton.

Size-exclusion experiments were performed using Varian Prostar chromatography equipment and followed standard protocols.¹⁶

Results and Fitting Procedures

Figure 3 shows typical experimental PFG NMR curves obtained from wet cotton fibers and linters with various probes. To extract quantitative information from these data that is widely accepted by the scientific community is difficult, time-consuming, and fraught with pitfalls. To optimize the procedure and ensure the conclusions are robust, the following fitting philosophy was adopted. For each probe the individual curves were fitted using the simplest acceptable model. The extracted values were interpreted and then the curves refitted with a model that better matched the situation. Finally a global fit of a probe's curve set was conducted to give fits with a single parameter set. Notably and most gratifyingly the conclusions did not substantially change between the three levels of fitting.

The simplest model that gave good fits to the data and was commensurate with the actual physical situation was the two-zone-exchange model of Kärger.²¹ For the cotton system, this corresponds to molecules in the water surrounding the fiber and molecules inside the fiber, with exchange between these two zones.



The residence time of a molecule in the two areas are τ_1 and τ_2 for water and cotton, respectively, and analogously the

TABLE 1: Best Fit Parameter Using the Kärger Model^a

probe	Δ/ms	$D_2/\text{m}^2 \text{ s}^{-1}$	$R/\mu\text{m}$	τ_1/s	τ_2/s
H ₂ O	49	1.5×10^{-10}	3.4	0.090	0.016
$D_1 = 1.9 \times 10^{-9} \text{ m}^2 \text{ s}^{-1}$	249	2.2×10^{-11}		0.17	0.051
$d = 0.23 \text{ nm}$	449	1.2×10^{-11}		0.21	0.079
	1000	5.5×10^{-12}		0.34	0.15
PEG200	14 ^b	1.3×10^{-10}	2.2		
$D_1 = 3.9 \times 10^{-10} \text{ m}^2 \text{ s}^{-1}$	24 ^b	1.1×10^{-10}			
$d = 1.11 \text{ nm}$	44	3.9×10^{-11}		0.088	0.021
	104	2.0×10^{-11}		0.13	0.037
	504	7.6×10^{-12}		0.18	0.11
PEG1500	44	1.8×10^{-11}	1.6	0.12	0.022
$D_1 = 1.2 \times 10^{-10} \text{ m}^2 \text{ s}^{-1}$	104	6.5×10^{-12}		0.15	0.034
$d = 3.64 \text{ nm}$	504	5.0×10^{-12}		0.52	0.15
	904	1.5×10^{-12}		0.54	0.20
PEG8000	44	3.3×10^{-12}	0.62	0.12	0.016
$D_1 = 3.2 \times 10^{-11} \text{ m}^2 \text{ s}^{-1}$	104	1.1×10^{-12}		0.19	0.029
$d = 6.00 \text{ nm}$	504	5.7×10^{-13}		0.5	0.13
	904	2.7×10^{-13}		0.40	0.17
PEG20000	44 ^b	6.6×10^{-12}	0.68		
$D_1 = 1.4 \times 10^{-11} \text{ m}^2 \text{ s}^{-1}$	104	1.1×10^{-12}		0.17	0.025
$d = 9.20 \text{ nm}$	504	5.1×10^{-13}		0.49	0.11
	904	3.3×10^{-13}		0.64	0.18
H ₂ O (linters)	49	2.8×10^{-11}		0.043	0.012
$D_1 = 1.9 \times 10^{-9} \text{ m}^2 \text{ s}^{-1}$	249	6.6×10^{-11}		0.16	0.057
$d = 0.23 \text{ nm}$	449	3.0×10^{-11}		0.16	0.079
	1000	5.7×10^{-11}		0.48	0.20

^a Probe diameters, d , are taken from ref 16. R values are the effective cage radii calculated from D_2 using eq 11. All values are for cotton fibers unless indicated. ^b Nonexchanging fits.

diffusion coefficients are D_1 and D_2 . In this case the net signal attenuation is given by

$$E_{\Delta}(g) = p'_1 \exp(-\gamma^2 \delta^2 g^2 D'_1 \Delta_r) + p'_2 \exp(-\gamma^2 \delta^2 g^2 D'_2 \Delta_r) \quad (2)$$

where

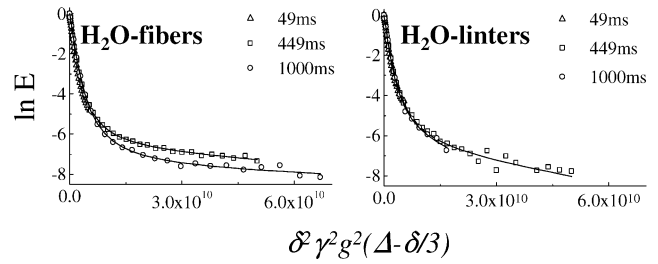
$$D'_1, D'_2 = \frac{1}{2} \left\{ D_1 + D_2 + \frac{1}{\gamma^2 \delta^2 g^2} \left(\frac{1}{\tau_1} + \frac{1}{\tau_2} \right) \mp \left[\left\{ D_2 - D_1 + \frac{1}{\gamma^2 \delta^2 g^2} \left(\frac{1}{\tau_2} - \frac{1}{\tau_1} \right) \right\}^2 + \frac{4}{\gamma^4 \delta^4 g^4 \tau_1 \tau_2} \right]^{1/2} \right\} \quad (3)$$

with D'_1 corresponding to the $-$ sign and D'_2 to the $+$. Additionally

$$p'_2 = \frac{1}{D'_2 - D'_1} (p_1 D_1 + p_2 D_2 - D'_1) \quad (4)$$

$$p'_1 = 1 - p'_2 \quad (5)$$

where γ is the magnetogyric ratio (42.57 MHz T⁻¹ for ¹H), δ is the total duration of gradient application for each bipolar pair (Figure 2) and was constant at 2.5 ms throughout these measurements, and $\Delta_r = (\Delta - \delta/3)$ is a simple reduced diffusion time, designed to give a first-order compensation for the finite duration, δ , of the gradient pulses (more advanced corrections make a negligible difference). D_1 may be estimated from the plots, Figure 3, as the initial gradient of the curves,¹⁴ and this gave values that were identical to those in simple aqueous solution.²² Therefore to reduce the number of variable parameters, D_1 was set to the measured value for free diffusion in aqueous solution. Fits were conducted in IDL (Research Systems Inc.), using a built-in fitting routine adapted from the Marquadt least-squares fitting algorithm.²³

**Figure 4.** Experimental signal attenuation curves and their fits to the Price model, eqs 7–10.

For some of the measurements with short Δ , no exchange could be observed and the curves were fitted instead using a simple biexponential (two-zone, nonexchanging) model:¹⁴

$$E_{\Delta}(g) = p_1 \exp(-\gamma^2 \delta^2 g^2 D_1 \Delta_r) + p_2 \exp(-\gamma^2 \delta^2 g^2 D_2 \Delta_r) \quad (6)$$

where p_1 and p_2 are the fractions of the two species with diffusion coefficients D_1 and D_2 , respectively. The results of the fits are displayed in Table 1.

Analysis of the results, vide infra, showed that the molecules within cotton fibers are trapped in cages. To confirm this conclusion, the modification of the Kärger model by Price²⁴ was used to refit the data. In this model, the diffusing probes in cotton are assumed to be confined in spherical cages of radius R . Here the net signal attenuation is again given by eq 2 but

$$D'_1, D'_2 = \frac{1}{2} \left\{ D_1 + \frac{1}{\gamma^2 \delta^2 g^2} \left(\frac{1}{\tau_1} + \frac{1}{\tau_2} \right) \mp \left[\left\{ D_2 + \frac{1}{\gamma^2 \delta^2 g^2} \left(\frac{1}{\tau_2} - \frac{1}{\tau_1} \right) \right\}^2 + \frac{4}{\gamma^4 \delta^4 g^4 \tau_1 \tau_2} \right]^{1/2} \right\} \quad (7)$$

and

$$p'_2 = \frac{1}{D'_2 - D'_1} (p_1 D_1 + p_2 D_2 - D'_1) \quad (8)$$

$$p'_1 = p_1 + p_2 + p'_2 \quad (9)$$

where

$$\hat{p}_2 = \left[\frac{3j_1(\gamma \delta g R)}{\gamma \delta g R} \right]^2 p_2 \quad (10)$$

in which $j_n(x)$ is a spherical Bessel function of the first kind.²⁵

Typical fits using the Price model are displayed in Figure 4, and the fit results given in Table 2. In the Price model it is assumed that Δ is long enough for the molecules to sample all points within the sphere before exchange occurs (i.e., slow exchange). This assumption is not justified at short Δ , and hence parameters extracted from these curves will be unreliable.

Global fits to the data sets were conducted for the fibers' data using the Price model and Kärger for the linters. These fits are shown in Figure 5, and values tabulated in Table 3. The radius values were restricted to $R < 10 \mu\text{m}$, as it would be physically unreasonable to have cages wider than the fiber diameter. Global fits were poorest with the water–fibers data set; this is to be expected, as the system is the most complex with H₂O in fibers being in the amorphous regions, in cages, and capable of cross-relaxation, vide infra. Consequently too many approximations spoil the fit and make the parameters derived from it least reliable.

There are several general problems to be born in mind in the fits of the current data. The system is somewhat difficult to

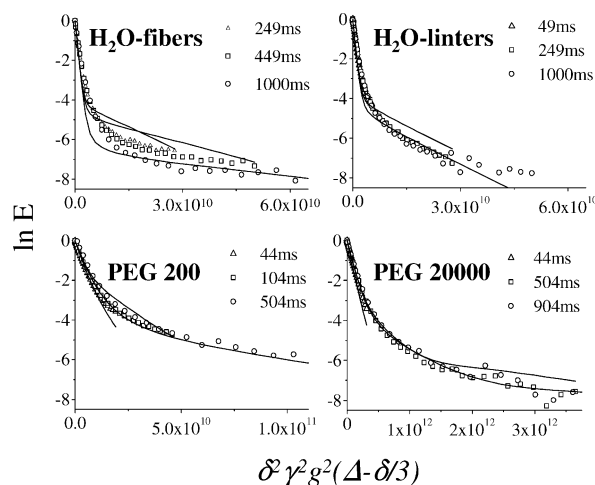


Figure 5. Experimental signal attenuation curves and their global fits to the Price model for threads and Kärger for linters.

TABLE 2: Best Fit Parameter Using the Price Model^a

probe	Δ/ms	$R/\mu\text{m}$	τ_1/s	τ_2/s
H ₂ O	49	13	0.092	0.023
$D_1 = 1.9 \times 10^{-9} \text{ m}^2 \text{ s}^{-1}$	249	5.1	0.16	0.050
$d = 0.23 \text{ nm}$	449	5.0	0.21	0.079
	1000	5.2	0.33	0.15
PEG200	14 ^b			
$D_1 = 3.9 \times 10^{-10} \text{ m}^2 \text{ s}^{-1}$	24 ^b			
$d = 1.11 \text{ nm}$	44	3.0	0.078	0.019
	104	3.2	0.12	0.034
	504	4.3	0.17	0.11
PEG1500	44	3.0	0.16	0.035
$D_1 = 1.2 \times 10^{-10} \text{ m}^2 \text{ s}^{-1}$	104	1.8	0.14	0.032
$D = 3.64 \text{ nm}$	504	3.6	0.51	0.15
	904	2.5	0.53	0.19
PEG8000	44	0.91	0.10	0.014
$D_1 = 3.2 \times 10^{-11} \text{ m}^2 \text{ s}^{-1}$	104	0.76	0.18	0.028
$d = 6.00 \text{ nm}$	504	1.1	0.48	0.12
	904	1.0	0.37	0.16
PEG20000	44 ^b			
$D_1 = 1.4 \times 10^{-11} \text{ m}^2 \text{ s}^{-1}$	104	0.80	0.15	0.02
$d = 9.20 \text{ nm}$	504	1.0	0.44	0.10
	904	1.2	0.62	0.17
H ₂ O (linters)	49	13.8	0.12	0.054
$D_1 = 1.9 \times 10^{-9} \text{ m}^2 \text{ s}^{-1}$	249	9.0	0.15	0.055
$d = 0.23 \text{ nm}$	449	7.9	0.15	0.076
	1000	17.0	0.46	0.11

^a All values for are for cotton fibers unless indicated. ^b Reasonable fits could not be obtained.

TABLE 3: Best Global Fit Parameters for Cotton Fibers Using the Price Model and for Cotton Linters Using the Kärger Model

probe	$R/\mu\text{m}$	τ_1/s	τ_2/s
H ₂ O-fibers	9.2	9.9	0.30
PEG200	5.7	0.35	0.13
PEG1500	3.7	2.3	0.29
PEG8000	1.3	8.5	0.34
PEG20000	2.5	2.4	0.33
H ₂ O-linters	$D_2 = 8.9 \times 10^{-11} \text{ m}^2 \text{ s}^{-1}$	9.7	0.34

study because of the nature of the diffusion regime in which the measurements are made. Spin–lattice relaxation of the sample magnetization imposes an upper limit on measurable diffusion times (Δ). In the range of diffusion times available, some of the probe molecules within cotton pass from completely unrestricted diffusion behavior (Kärger model) to completely restricted diffusion behavior (Price model). Probably, much of the data lie in an intermediate regime, where diffusion inside the fibers is partially restricted. Additionally, fitting is to discrete

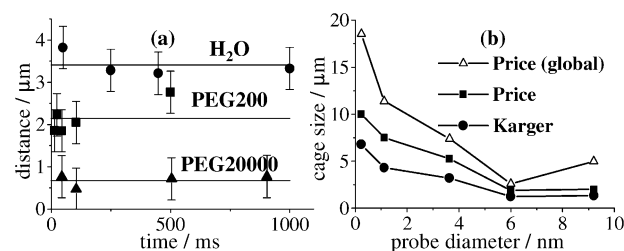


Figure 6. (a) Distance moved with time for three probes in wet cotton threads, according to Kärger model and eq 11. (b) Dependence of cage size (diameter) on probe diameter from the various methods used for fitting the data.

values of D_2 , R , τ_1 , and τ_2 , although in reality a distribution of cage sizes and exchange times will exist, as is indeed shown by the variation in R with probe size. It is not clear that these distributions are equally sampled at varying Δ ; for example it would be expected that the faster exchange areas would have a greater influence on the measurements at short Δ . Finally, models that are very sensitive to their parameters are fitted to relatively noisy data with variable signal-to-noise ratio across the data sets (due to different number of samples).²⁶ These factors mean that the strategy of globally fitting the data may not be appropriate. Therefore all three fit methods are discussed in the interpretation section.

Interpretation

(a) Diffusion Coefficients. (i) *Cotton Fibers.* In cotton fibers the measured diffusion coefficients, D_2 , obtained from the Kärger fit, decreased with time for all the probes, Table 1. This behavior is not expected for a simple two-zone exchange model, and consequently the macrostructure of the fiber must restrict the intrafiber diffusion in some way. The simplest explanation is that the probes are trapped in cages within the fiber; as the time increases, the probes do not move any further, thus giving an apparent decrease in D_2 . If this is the case, then the distance moved, d , by the probe molecule in a time, t , estimated by

$$d = \sqrt{2Dt} \quad (11)$$

should be constant, as is found, Figure 6a. On average, the probe will have moved from the center of the cage to the wall, and hence a characteristic cage dimension is $2d$. The cage size decreases from 6.8 to 1.4 μm as the probes increased in diameter from 0.22 to 9.2 nm, Figure 6b. It is notable that changes in the nanometer dimensions of the probes alter the much larger micrometer dimensions of the cages.

In previous PFG work, Li et al.²⁷ measured a value of 8 μm using H₂O, for the cage dimensions in softwood cellulose fibers oversaturated with water, in good agreement with the above. Topgaard and Södermann²⁸ also found micrometer cages in wet wood fibers. For fibers with much lower water content they found larger dispersion than those observed here.²⁹ They interpreted this result in terms of proton exchange between the water and cellulose, leading to cross-relaxation. The high water content of the current samples means that cross-relaxation effects may be neglected to a first approximation, as it will be too slow.³⁰ Furthermore, the PEGs are not capable of proton exchange yet still show the same caging effects as H₂O. If proton exchange was dominant, then H₂O in fibers and linters should give identical results, as both mediate exchange; however the results are clearly different, vide infra.

It should be noted that Harding et al.³¹ has reported global fits of water in a cardboard sample using the Kärger model,

without the use of caging. However Harding's sample contained cellulose from woods of various qualities and various trees, as well as filler material of unknown origin, making comparisons impossible.

It may be argued that the caging conclusion is invalid, as the Kärger model and the above analysis is not a good approximation in this case. However the data were well fitted with the Price model, in which the cotton is considered as a cage and gave similar cage size, Table 2 and Figure 6b. For example for H₂O and PEG20000, cage diameters ($2R$) of 10 and 2 μm , respectively, are obtained with the Price fits and 6.8 and 1.4 μm using Kärger. As would be expected, these diameters are independent of measurement time except at short Δ , where R rises; however as already noted, the Price model fails at short Δ because there is not enough time to sample the cage walls. Global fitting of the PFG curves gave slightly larger values for R , Table 3 and Figure 5b, but the same dependence on probe diameter.

To keep the discussion lucid, only one set of cage data is discussed below. The Kärger approach is used, as it can be applied to all the curves whatever the values of Δ .

The cage volumes, estimated as spheres, vary from 1.4 (PEG20000) to 165 μm^3 (water). The smallest unit in cotton that could constitute a cage is the microfibril; however its volume of 0.1 μm^3 is too small.^{2,3} The growth rings of the fiber are another alternative and are typically 0.1–0.5 μm in width, 5 μm in diameter, and 1–5 mm in length, giving volumes of 3000–70 000 μm^3 , which are too large. However the growth rings are constructed from the microfibrils arranged in spirals, the direction of which reverses 50 times along its length, Figure 1,³² producing subunits of 60–1400 μm^3 , in reasonable agreement with the measured value for water. Between consecutive growth rings there are empty spaces that fill with water.³² These spaces are of dimensions similar to the growth rings, and to distinguish between these two possibilities, note must be taken of the absolute values of D_2 at shortest diffusion time (smallest Δ). If measurements are made before the probe hits the cage wall, then the D_2 will be the probe's diffusion coefficient in the medium filling the cage and this is the highest value of D_2 that can be measured. If the cage is situated between the growth rings, a diffusion coefficient similar to that in free water would be expected. Alternatively if it is actually in the growth ring, a much higher value would be expected, as the probe would be moving in the amorphous regions, which are tortuous and have increased viscosity due to being in a polysaccharide/water mix,⁸ vide infra. It is probable that for even the shortest diffusion time measurements many of the molecules have reached the cage walls, even so D_2 approaches the corresponding value in water. The earliest measurement was at 14 ms with PEG200, giving $D_2 = 1.3 \times 10^{-10} \text{ m}^2 \text{ s}^{-1}$, only 3 times smaller than the value in D₂O, $3.9 \times 10^{-10} \text{ m}^2 \text{ s}^{-1}$. These values are too large for diffusion in the amorphous regions, and therefore the cages observed are assigned to be the spaces between the growth rings.

The cage walls are the fiber growth rings, including cellulose protruding from the ring into the space, and clearly access to the cages and connection between cages will be through these walls. The growth rings are constructed from microfibrils, which contain nanopores in the range 1–5 nm.¹⁶ Clearly larger PEGs are size-excluded from these pores, and this restriction could reduce the effective volume and connectivity of the cages.

The nanopore distribution in the fiber growth rings may be measured by size-exclusion chromatography,¹⁶ and the results from this experiment on the cotton used here are shown in Figure 7. There is a remarkable agreement between the NMR results,

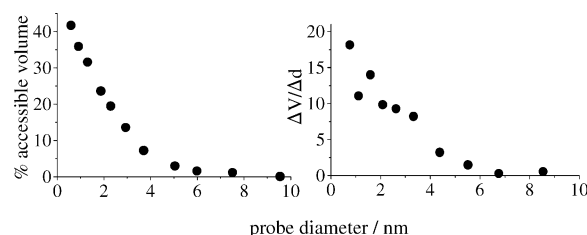


Figure 7. (a) Volume of cotton fiber accessible to PEGs of different diameters measured by size-exclusion chromatography. (b) Pore size distribution displayed as the % volume available per pore diameter ($\Delta V/\Delta d$).

Figure 6b, and size exclusion, Figure 7, strongly supporting the conclusion that dependence of cage size on probe size is due to size-exclusion effects. The effect of probe size on the total accessible volume is discussed in section b(i).

(ii) *Cotton Linters.* Cotton fibers used in cloth are the long fibers of the cotton plant, whereas cotton linters are the much shorter fuzz fibers. One would expect that the shorter length would lead to an opening of the cages, as each "cage" is near the end of the fiber, where access is not restricted. In this case the water between the growth rings would appear as free and should allow observation of the smaller amount of slow moving water in the amorphous regions.^{4,7,8} (From literature values³ in wet cotton approximately 10% of the water in the fiber is in the amorphous region and 90% between the growth rings.) The results agree with the supposition, Table 1, as in linters D_2 is not time dependent and has a value of 4.5×10^{-11} or $8.9 \times 10^{-11} \text{ m}^2 \text{ s}^{-1}$ from the global Kärger fit. This is supported by the Price model, which does not give a stable cage radius R . The values increase with time, Table 2, as would be expected, when trying to fit a cage size to free diffusion.

The microviscosity of the amorphous region is approximately 10 cP,⁸ from which a value of $1.9 \times 10^{-10} \text{ m}^2 \text{ s}^{-1}$ may be calculated for D_2 using

$$D_{\text{calc}} = kT/3\pi\eta d \quad (12)$$

The disparity between the calculated and measured values is assigned to the tortuosity, T , which can be conveniently defined as³³

$$T = D_{\text{calc}}/D_{\text{measured}} \quad (13)$$

and gives a value of $T = 2$ –4 (global and average value from individual fits). Water moving within the amorphous regions must diffuse around the crystallites, thereby adding to the distance that must be covered for a net displacement. For the 5–7 by 9–12 nm rectangular crystallites in cotton linters^{2,3} this effect would decrease the measured D_2 by a factor of 1.6–3.4 compared to that predicted by the microviscosity. Further decreases may occur because the water can absorb onto the crystallite surface, slowing displacement without affecting the microviscosity.⁶ Consequently the measured $T = 2$ –4 is in very good agreement with prediction for cotton. Interestingly it is also close to that seen in other nanoporous media such as rock; for example, measured values of tortuosity by both PFG NMR and electrical conductivity are 3.4 and 7.7 for sandstone and limestone, respectively.³³

(b) *Residence Times.* (i) *Cotton Fibers.* The residence times, τ_1 and τ_2 , increase with time until approximately 500 ms and then become constant within experimental error for the individual fits, Table 1 and Table 2. This behavior is expected simply because at shorter diffusion times the exchange times are longer than Δ and therefore cannot be sampled properly.

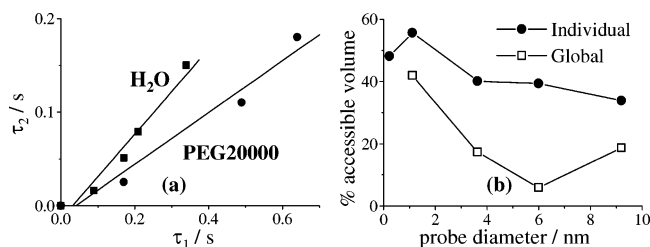


Figure 8. (a) Linear dependence of τ_1 on τ_2 from which the ratio τ_1/τ_2 is calculated. As both Kärger and Price give identical τ values, only one set is shown. (b) Variation in accessible volume with probe diameter, calculated from eq 15, using data from the individual and global fits.

Once Δ is longer than τ_1 and τ_2 , stable values can be measured within experimental error. The τ_2 values obtained from the global fits, Table 3, are very similar to those from the individual fit approach; however the τ_1 values are in general much larger. Notably many of the τ_1 values obtained globally are much larger than the longest sampling period (1 s), which appears odd. Expediently, for all but the water-fibers data the differences only change the quantitative but not qualitative conclusions. As already mentioned, the water fits are the poorest, probably due to the system being the most complex. From the size exclusion and previous work^{2,3,16} τ_1/τ_2 values similar to PEG200 would be expected, as indeed are found in the individual fits. Hence the global value for τ_1 water looks suspicious and is neglected.

For equilibrium conditions the amount of material moving in and out of the two regions must be equal, so that

$$\frac{w_1}{\tau_1} = \frac{w_2}{\tau_2} \quad (14)$$

where w_1 and w_2 are the weights of material in the two regions and $w_1 + w_2 = W$ is the total weight of material applied. Consequently, the fraction of material in the cotton is calculated from the ratio of the residence times and W via

$$w_2 = \frac{\tau_2}{\tau_1 + \tau_2} W \quad (15)$$

For larger probe molecules a smaller fraction would be expected in cotton due to size-exclusion effects, such as seen in Figures 6 and 7. To calculate w_2 , only the ratio of τ_1/τ_2 is required, which is most accurately obtained from the individual fit data, Table 1 and 2, by plotting all the fitted values, Figure 8a. For the global data, Table 3, simple division is all that is required. w_2 may be converted into the % accessible hydrated cotton volume, simply by multiplying by the density of cellulose (1.55 g/mL), which is plotted in Figure 8b.

For H₂O and PEG200 ~50% of the hydrated cotton volume is accessible, in agreement with literature values of 50% for the water content of saturated cotton fibers.³ For the larger PEGs this falls to ~20–30%, due to size exclusion and is a surprisingly small change considering that the cage size drops from 6.8 to 1.4 μm . This disparity may be accounted for by the morphology and connectivity of the cages. Consider a simple one-dimensional 3 μm cage subdivided into three 1 μm subcages. If the pathway between the subcages is 2 nm wide, then it will be seen as one 3 μm cage by H₂O and PEG200 but three 1 μm cages by the larger PEGs, although the total cage volume does not alter. In other words, smaller probes will see the same space as a larger cage, because they can freely move between the smaller subcages seen by the large probes. From the results roughly half of the cages become completely

inaccessible to the larger PEGs due to their size preventing any access. The reader is reminded this is the accessible volume in the space between the growth rings, not the accessible volume in the amorphous regions of the growth rings measured by size exclusion, Figure 7.

Of the two τ values, τ_2 is the easiest to interpret, as for a water-saturated fiber, w_2 and hence τ_2 are fixed. For the asymptotic values from the individual fits, Tables 1 and 2, and the global values, Table 3, τ_2 does not greatly alter between the probes, with an average value of 0.2 s. As the τ_2 does not change with probe, the exit process cannot be diffusion controlled, and consequently an energy barrier must be overcome to move from cotton to free water. In this case the rate constant for escape, $k_{\text{esc}} (=1/\tau_2)$ can be described by the Arrhenius equation:

$$k_{\text{esc}} = Ae^{-E_A/RT} \quad (16)$$

For a simple unimolecular process the frequency factor, A , in the Arrhenius equation is typically 10^9 – 10^{12} s^{-1} ,³⁴ giving an activation energy, E_A , of 48–65 kJ mol⁻¹ for $k_{\text{esc}} = 5 \text{ s}^{-1}$. A hydrogen bond in cotton² has an energy of 25 kJ mol⁻¹, close to the estimated value for E_A , and it would seem reasonable that weak hydrogen bonds present a barrier to exit and entry into the cotton structure. These bonds will clearly be present in the amorphous regions and are consistent with all access being via these regions. Hence, cotton fibers are quite leaky tubes, with the majority of access into the fiber being through the walls not via the fiber ends.

(ii) *Cotton Linters.* Application of eq 15 using the individual data values, Table 1, showed that 55% of the cotton linters volume was accessible to water. This value is too large, as the maximum amount of water in the amorphous regions can only be 10%, although the total water retention value is 40%.^{2,3} Using the value of τ_2/τ_1 from the global fits gives a value of 7% accessibility, much closer to that expected. As linters represent the simplest system studied, matching the Kärger assumption well, it may be expected that the global fit should give the better values, as observed.

Interestingly the value of τ_2 does not greatly change between fibers and linters, which means that the exit of molecules (and hence entry) into the two structures is controlled by the same factors. This is expected, as both have identical nanostructure which will control the exit/entry process. However the morphology of the microstructure is different, producing cages in fibers but not linters.

Conclusion

PFG NMR study of cotton fibers and linters using water and PEGs as probes has revealed several interesting new insights. In cotton fibers, micrometer-sized cages are observed, the size of which decreases as the nanometer size of the probe increases. This result may be rationalized by the cages being between the growth rings of the fiber with access via the amorphous regions of the ring walls. Separate size-exclusion experiments show that the pore size of the amorphous region is between 1 and 5 nm, in good agreement with the supposition. In the much shorter cotton linters there are no cages, and the results give the effective diffusivity and tortuosity in the amorphous regions. Access in/out of fibers and linters requires an activation energy of roughly 50 kJ mol⁻¹, consistent with hydrogen bonding providing the barrier.

The work has highlighted some of the strengths and weaknesses of PFG NMR when applied to relatively complicated

systems such as cotton. It perhaps brings into focus the need for more theoretical work on the best means to fit such data.

Acknowledgment. Dr. J. van Duynhoven and Dr. G.-J. Goudappel (Unilever Research, Vlaardingen) are thanked for help with the pulse sequences. Ms. J. Williams and Mr. J. LeDuc (Unilever Research Port Sunlight) are thanked for performing the size-exclusion measurements. Unilever Research Port Sunlight is thanked for financial support and encouragement. Mr. A. H. Batchelor (Newcastle) is thanked for discussions on data fitting. Prof. Price (Tokyo) and Prof. Kärger (Leipzig) are thanked for useful comments on the applicability of their models.

References and Notes

- (1) Lamgley, P. J.; Hulliger, J. *Chem. Soc. Rev.* **1999**, 28, 279.
- (2) Krässig, H. A. *Cellulose*; Gordon Breach Science Publishers: Amsterdam, 1993.
- (3) Klemm, D.; Philipp, B.; Heinze, T.; Heinze, U.; Wagenknecht, W. *Comprehensive Cellulose Chemistry Volume 1*; Wiley-VCH: Weinheim 1998.
- (4) Batchelor, S. N. *J. Phys. Chem. B* **1999**, 103, 6700.
- (5) Batchelor, S. N.; Shushin, A. I. *J. Phys. Chem. B* **2001**, 105, 3405.
- (6) Scheuermann, R.; Roduner, E.; Batchelor, S. N. *J. Phys. Chem. B* **2001**, 105, 11474.
- (7) Batchelor, S. N.; Shushin, A. I. *Appl. Magn. Reson.* **2002**, 22, 47.
- (8) Hunt, P.; Worrall, D. R.; Wilkinson, F.; Batchelor, S. N. *J. Am. Chem. Soc.* **2002**, 124, 8532.
- (9) Kono, H.; Yunoki, S.; Shikano, T.; Fujiwara, M.; Erata, T.; Takai, M. *J. Am. Chem. Soc.* **2002**, 124, 7506 and 7512.
- (10) Vietor, R.; Newman, R.; Ha, M.; Apperley, D.; Jarvis, M. *Plant J.* **2002**, 30, 721.
- (11) Hediger, S.; Lesage, Emsley, L. *Macromolecules* **2002**, 35, 5078.
- (12) Capitani, D.; Proietti, N.; Ziarelli, F.; Segre, A. *Macromolecules* **2002**, 35, 5536.
- (13) Furo, I.; Daicic, J. *Nordic Pulp Paper Res. J.* **1999**, 14, 221.
- (14) Callaghan, P. T. *Principles of Nuclear Magnetic Resonance Microscopy*; Clarendon Press: Oxford, 1997.
- (15) Maunu, S. *Prog. NMR Spectrosc.* **2002**, 40, 151.
- (16) Brederick, K.; Gruber, M.; Otterbach, A.; Schulz, F. *Textilveredlung* **1996**, 31, 194.
- (17) Cotts, R. M.; Hoch M. J. R.; Sun, T.; Marker, J. T. *J. Magn. Reson.* **1989**, 83, 252.
- (18) Gibbs, S. J.; Johnson, C. S. *J. Magn. Reson.* **1991**, 93, 395.
- (19) Li, T. Q.; Henriksson, U.; Klason, T.; Ödberg, L. *J. Colloid Interface Sci.* **1992**, 154, 305.
- (20) Nestle, N.; Qadan, A.; Galvosas, P.; Suss, W.; Kärger, J. *Magn. Reson. Imaging* **2002**, 20, 567.
- (21) Kärger, J. *Adv. Colloid Interface Sci.* **1985**, 23, 129.
- (22) Holz, M.; Heil, S. R.; Sacco, A. *Phys. Chem. Chem. Phys.* **2000**, 2, 4740.
- (23) After the routine CURFIT in: Bevington, P. R.; Robinson, D. K. *Data Reduction and Error Analysis for the Physical Sciences*, 3rd ed.; McGraw-Hill: New York, 2001.
- (24) Price, W. S.; Barzykin, A. V.; Hayamizu, K.; Tachiya, M. *Biophys. J.* **1998**, 74, 2259.
- (25) Abramowitz, M.; Stegun, I. A. *Handbook of Mathematical Functions*; Dover: New York, 1970.
- (26) Batchelor, A. H.; Green, G.; Woods, W. *Automatica*, submitted.
- (27) Li, T.-Q.; Häggkvist, M.; Ödberg, L. *Langmuir* **1997**, 13, 3570.
- (28) Topgaard, D.; Södermann, O. *Cellulose* **2002**, 9, 139.
- (29) Topgaard, D.; Södermann, O. *Langmuir* **2001**, 17, 2694.
- (30) Reference 28 gives $\tau(\text{exchange})$ for cellulose of 45 ms. Assuming each glucose monomer of the polysaccharide has one proton available for exchange and a surface area of 1 nm², then 1 g of cotton (surface area = 160 m² g⁻¹) exchanges 6×10^{-3} mol of water per second, or 0.1 g s⁻¹, smaller than water contents of current samples, 1.1–1.3 g g⁻¹.
- (31) Harding, S. G.; Wessman, D.; Stenström, S.; Kenne, L. *Chem. Eng. Sci.* **2001**, 56, 5269.
- (32) Hearle, J. W. S.; Peters, R. H. *Fibre Structure*; Butterworth: Manchester, 1963.
- (33) Mair, R. W.; Wong, G. P.; Hoffmann, D.; Hürlimann, M. D.; Patz, S.; Schwartz, L. M.; Walsworth, R. L. *Phys. Rev. Lett.* **1999**, 83, 3324.
- (34) Benson, S. W. *Thermochemical Kinetics*, 2nd ed.; John Wiley and Sons: New York, 1976.